PNAS
www.pnas.org

Supplementary Information for

Minimal gene set from *Sinorhizobium (Ensifer) meliloti* pSymA required for efficient symbiosis with *Medicago*

Barney A. Geddes, Jason Kearsley, Jiarui Huang, Maryam Zamani, Zahed Muhammed, Leah Sather, Aakanx Panchal, George C. diCenzo, and Turlough M. Finan**.**

Turlough M. Finan
Email: finan@mcmaster.ca

This PDF file includes:

Table S1. Summary of symbiotic data for major checkpoints of *S. meliloti* pSymA genome reduction.

Strain	**Description**	***Medicago sativa***				***Medicago truncatula***			***Melilotus officinalis***		
		Shoot dry weight (mg)	Nodule number	Nodule fresh weight (mg)	Acetylene reduction*	Shoot dry weight	Nodule number	Nodule fresh weight (mg)	Shoot dry weight	Nodule number	Nodule fresh weight (mg)
RmP110	Wildtype	64.7 (12.5)	5.0 (0.6)	3.7 (0.7)	+ 1859 (240)	34.4 (2.4)	8.9 (2.0)	1.4 (0.3)	82.8 (22.5)	8.3 (2.2)	5.9 (1.0)
RmP4253	ΔpSymA	8.4 (0.9)	0	0	-	13.0 (2.0)	0	0	2.9 (0.9)	0	0
RmP4291	ΔpSymA minSymA1.0	72.3 (28.9)	8.3 (0.7)	4.5 (1.2)	+ 2350 (410)	36.8 (9.1)	7.8 (1.3)	1.6 (0.4)	58.3 (23.0)	9.2 (1.0)	3.9 (1.1)
RmP4600	ΔpSymA minSymA2.1	60.6 (10.9)	14.8 (3.7)	1.5 (0.4)	+ 2473 (1153)	27.9 (4.1)	13.2 (0.8)	0.8 (0.4)	81.2 (21.6)	10.7 (1.8)	3.6 (0.7)
RmP4663	ΔpSymA minSymA3.2	35.3 (5.7)	8.1 (4.3)	2.2 (0.6)	+ 1574 (822)	24.6 (2.6)	5.7 (1.5)	2.3 (1.6)	68.1 (14.9)	8.4 (1.6)	5.2 (0.9)
RmP4621	ΔpSymA minSymA3.3	41.6 (5.8)	ND	ND	+ 696 (192)	16.6 (3.0)	ND	ND	56.6 (20.1)	ND	ND
Uninoculated control		7.6 (2.1)	0	0	-	11.4 (1.2)	0	0	3.3 (1.0)	0	0

* The detection of ethylene production by acetylene reduction assay is indicated as + (detected ethylene production) or – (ethylene production was not detected). The actual values measured are included below and expressed as nmoles ethylene producted $hour^{-1}$ $plant^{-1}$.

Data are from 3 independent replicates (pots) with 6 plants per pot (*M. sativa*) and 4 plants per pot (*M. truncatula* and *M. officinalis*) and were collected 31 days post inoculation. Shoot dry weight and nodule number are calculated per plant, and nodule fresh weight is calculated from average fresh weight per nodule. Values in parentheses indicate standard deviation of the mean. ND indicates no data collected.

Table S2. Strains and plasmids used in this study

Strain	Description	Reference
Sinorhizobium meliloti		
Rm1021	SU47 *str*-21; Sm^R	Meade et al. 1982
RmG340	Rm1021 *phe32*:Tn*5*-233	Oresnik et al. 1994
RmP110	Wildtype, Rm1021 with wild type *pstC*; Sm^R	Yuan et al. 2006
RmP991	RmP110, ΔA116 (pSymA nt. 313,654-458,916) (pTH1944); Sm^R Tc^R	Milunovic et al. 2014
RmP938	RmP110 with pTH1522 (nt 400,267–402,136), pTH1937 (nt 458,916-459,668) integrated in pSymA ; Sm^R Nm^{R*} Gm^R	Milunovic et al. 2014
RmP939	RmP110, ΔA117 (pSymA nt. 402,136-458,916) (pTH1944); Sm^R Tc^R	Milunovic et al. 2014
RmP941	RmP110, ΔA118 (pSymA nt. 459,668-505,335) (pTH1944); Sm^R Nm^R Gm^R Tc^R	Milunovic et al. 2014
RmP946	RmP110 with pTH1522 (nt 623673–624863), pTH1937 (nt 677,157-678,150) integrated in pSymA; Sm^R Nm^R Gm^R	Milunovic et al. 2014
RmP947	RmP110, ΔA121 (pSymA nt. 624,863-677,157) (pTH1944); Sm^R Tc^R	Milunovic et al. 2014
RmP1615	*metH*::Tn5; methionine auxotroph	Laboratory collection
RmP1685	RmP110 Ω *attB* Ω ΦC31 *int*; Sm^R Nm^R	diCenzo et al. 2014
RmP2201	RmP110 *manB*(SMc04255) replaced by FRT-kan-FRT; Sm^R, Nm^R	Katerine Kibitkin Msc Thesis
RmP2227	RmP110 *manB*(SMc04255):FRT Sm^R	Katerine Kibitkin Msc Thesis
RmP2667	RmP110 Ω *attB* Ω ΦC31 *int* (pTH1944); Sm^R Tc^R	diCenzo et al. 2013
RmP2507	RmP110 *hypRE*:FRT-*kan*-FRT; Sm^R Nm^R	White et al. 2012
RmP3543	RmP110 ΔA301 (pSymA nt. 507,388-623,673) (pTH2505); Sm^R Gm^R Tc^R	diCenzo et al. 2016
RmP4218	RmP3543 with pTH2505 plasmid cured; Sm^R Gm^R	This work
RmP4219	RmP4218 with ΔA301 scar removed with pTH3237; Sm^R	This work
RmP4247	RmP110 with pSymA cured, Sm^R	This work
RmP4250	RmP4247 with *hypRE*:FRT-*kan*-FRT introduced from RmP2507; Sm^R Nm^R	This work
RmP4253	RmP4250 with pTH2505 introduced and *kan* cassette flipped out by Flp/FRT *hypRE*:FRT; Sm^R Tc^R	This work
RmP4291	minSymA1.0; RmP4253 with pTH3255 integrated into *hypRE*:FRT; Sm^R Gm^R Nm^R	This work
RmP4307	RmP4219 with pTH1522 (nt 400,267–402,136) integrated in pSymA; Sm^R Gm^R	This work
RmP4308	RmP4219 with pTH1937 (nt 677,157-678,150) integrated in pSymA; Sm^R Nm^R	This work
RmP4309	RmP4219 with pTH1522 (nt 400,267-402,136) and pTH1937 (nt 677,157-678,150) integrated in pSymA; Sm^R Gm^R Nm^R	This work
RmP4310	RmP4309 carrying pTH2505; Sm^R Gm^R Nm^R Tc^R	This work
RmP4346	RmP4253 with pTH3278 (fix-1) integrated into *hypRE*:FRT; Sm^R Nm^R	This work
RmP4347	RmP947 with pTH1944 removed by pBBRMCS5 incompatibility; Sm^R Gm^R	This work
RmP4371	minSymA2.0; RmP4253 with pTH3294 integrated into LP-B1 (*hypRE*:FRT); Sm^R Nm^R	This work
RmP4372	RmP110 with pTH3311 integrated; Sm^R Nm^R	This work
RmP4373	RmP110 with pTH3312 integrated; Sm^R Nm^R	This work

RmP4374	RmP110 with pTH3313 integrated; Sm^R Nm^R	This work
RmP4375	RmP110 with pTH3314 integrated; Sm^R Nm^R	This work
RmP4376	RmP4372 with pTH3315 integrated; Sm^R Gm^R Nm^R	This work
RmP4377	RmP4373 with pTH3316 integrated; Sm^R Gm^R Nm^R	This work
RmP4378	RmP4374 with pTH3317 integrated; Sm^R Gm^R Nm^R	This work
RmP4379	RmP4375 with pTH3318 integrated; Sm^R Gm^R Nm^R	This work
RmP4436	RmP4373 with pTH3318 integrated; Sm^R Gm^R Nm^R	This work
RmP4437	RMP4374 with pTH3318 integrated; Sm^R Gm^R Nm^R	This work
RmP4483	ΦRmP4346 (fix-1) → RmP4347 (ΔA121); Sm^R Gm^R Nm^R	This work
RmP4503	RmP110 with pTH3364 integrated; Sm^R, Gm^R	This work
RmP4504	RmP110 with pTH3365 integrated; Sm^R, Gm^R	This work
RmP4505	RmP4503 with *gusA* integrated and pTH3364 backbone removed via *sacB* Sm^R	This work
RmP4506	RmP14505 with *celB* integrated and pTH3365 backbone removed via *sacB*; Sm^R	This work
RmP4507	ΦRmP340 (*phe32*::Tn*5*-233) → RmP4291; ; Sm^R Gm^R Nm^R Sp^R	This work
RmP4508	ΦRmP4505 (*gusA*)→ RmP4507; Sm^R Gm^R Nm^R	This work
RmP4509	ΦRmP4506 (*celB*)→ RmP4507; Sm^R Gm^R Nm^R	This work
RmP4512	RmP110, ΔA401 (pSymA nt 400,267-423,453) via pTH2505; Sm^R, Gm^R	This work
RmP4513	RmP110, ΔA402 (pSymA nt 423,454-465,115) via pTH2505; Sm^R, Gm^R	This work
RmP4514	RmP110, ΔA403 (pSymA nt 465,116-476,084) via pTH2505; Sm^R, Gm^R	This work
RmP4515	RmP110, ΔA404 (pSymA nt 476,085-507,338) via pTH2505; Sm^R, Gm^R	This work
RmP4516	RmP110, ΔA405 (pSymA nt 423,454-507,338) via pTH2505; Sm^R, Gm^R	This work
RmP4517	RmP110, ΔA406 (pSymA nt 465,116-507,338) via pTH2505; Sm^R, Gm^R	This work
RmP4523	ΦRmP4371 (minSymA2.0) → RmP110 (wildtype)	This work
RmP4524	ΦRmP4371 (minSymA2.0) → RmP4512 (ΔA401)	This work
RmP4525	ΦRmP4371 (minSymA2.0) → RmP4512 (ΔA403)	This work
RmP4526	ΦRmP4371 (minSymA2.0) → RmP4512 (ΔA403)	This work
RmP4527	ΦRmP4371 (minSymA2.0) → RmP4512 (ΔA404)	This work
RmP4528	ΦRmP4371 (minSymA2.0) → RmP4512 (ΔA405)	This work
RmP4529	ΦRmP4371 (minSymA2.0) → RmP4512 (ΔA406)	This work
RmP4532	RmP2667 with pTH3372 (fix-2) integrated into LP-C1 via *attB*; Sm^R Sp^R Tc^R	This work
RmP4597	minSymA3.0; RmP4253 with pTH3375 integrated into LP-B1 (*hypRE*:FRT)	This work
RmP4598	RmP4253 with pTH3376 integrated into LP-B1 (*hypRE*:FRT)	This work
RmP4599	minSymA3.1; ΦRmP4532 (fix-2) → RmP4597 (minSymA3.0); Sm^R Nm^R Sp^R	This work
RmP4600	minSymA2.1; ΦRmP4532 (fix-2) → RmP4371 (minSymA2.0); Sm^R Nm^R Sp^R	This work
RmP4608	ΦRmP4532 → RmP4603; Sm^R Nm^R Sp^R	This work
RmP4610	ΦRmP4532 → RmP4605; Sm^R Nm^R Sp^R	This work
RmP4612	RmP1685 with pTH3373 (synth-nif) integrated into LP-C1 via *attB*	This work
RmP4613	ΦRmP4612 (synth-nif) → RmP4346 (fix-1); Sm^R Nm^R Tc^R	This work

RmP4614	ΦRmP4612 (synth-nif) → RmP4598 (synth-fix); Sm^R Nm^R Tc^R	This work
RmP4617	ΦRmP2201 (*manB*:FRT-kan-FRT) → RmP4247 (ΔpSymA)	This work
RmP4618	RmP2227 with pTH3371 (synth-nod) integrated into LP-C2 (*manB*:FRT) and transduced into RmP110; Sm^R Sp^R	This work
RmP4620	ΦRmP4618 (synth-nod) → RmP4613(fix-1/synth-nif); Sm^R Nm^R Sp^R Tc^R	This work
RmP4621	ΦRmP4618 (synth-nod) → RmP4614 (synth-fix/synth-nif); Sm^R Nm^R Sp^R Tc^R	This work
RmP4624	ΦRmP4532 (fix-2)→ RmP4512 (ΔA401); Sm^R Gm^R Sp^R	This work
RmP4628	ΦRmP4506 (*celB*)→ RmP4371 phe(-) (viaΦ RmG340 transduction); phe (+), Sm^R Nm^R	This work
RmP4629	ΦRmP4505 (*gusA*)→ RmP4371 phe(-) (viaΦ RmG340 transduction) ; phe (+), Sm^R Nm^R	This work
RmP4645	ΦRmP4532 (fix-2) → RmP4627 (minSymA2.0 *gusA*); Sm^R, Nm^R, Sp^R	This work
RmP4646	ΦRmP4532 (fix-2) → RmP4628 (minSymA2.0 *celB*); Sm^R, Nm^R, Sp^R	This work
RmP4657	RmP4617 with kan cassette removed by Flp recombinase (pTH2505); Sm^R, Tc^R	This work
RmP4658	RmP4657 with pTH3294 integrated (minSymA2.0) into *manB*:FRT (LP-C2); Sm^R, Nm^R	This work
RmP4661	RmP2667 with pTH3396 (reduced fix-2) integrated into LP-C1 via *attB*; Sm^R, Sp^R	This work
RmP4663	minSymA3.2; ΦRmP4661 (reduced fix-2) → RmP4597 (minSymA3.0); Sm^R Nm^R Sp^R	This work
RmP4684	ΦRmP4532 (fix-2) → RmP4658 (minSymA2.0:LP-C2), minSymA2.1 LP-C2; Sm^R, Nm^R, Sp^R	This work
RmP4737	RmP4657 with pTH3434 (NGR234 nod) integrated into LP-C1 via *attB*; Sm^R, Sp^R	This work
RmP4741	ΦRmP4737 (NGR234 nod) → RmP4614 (synth-nod/synth-nif); Sm^R, Nm^R, Sp^R, Tc^R	This work
Escherichia coli		
DH5α	*endA1 hsdR17 supE44 thi-1 recA1 gyrA96 relA1* Δ(*argF-lacZYA*) U169 φ80d*lacZ*ΔM15	Invitrogen
Epi300	F– *mcrA* Δ(*mrr-hsdRMS-mcrBC*) φ80d*lacZΔM15* Δ*lacX74 recA1 endA1 araD139* Δ(*ara, leu*)7697 *galU galK* λ^- *rpsL nupG trfA dhfr*; Sm^R Cm^R	Lucigen
M928	Rifampicin resistant DH5α; Rf^R	Lab collection
M2608	M928 with pTH3255; Rf^R Gm^R Km^R	This work
MT616	MM294A *recA-56* (pRK600), mobilizer; Cm^R	Finan et al. 1986
Saccharomyces cerevisiae		
VL6-48	MATα his3-Δ200 trp1-Δ1 ura3−52 lys2 289 ade2−1 met14 cir^0	ATCC® MYA-3666™
Plasmid	**Description**	**Reference**
pJQ200SK	Suicide vector for *sacB*-mediated double homologous recombination; Gm^R	Quandt and Hynes 1993
pOGG024	pBBR1 Golden Gate cloning plasmid; Gm^R	Geddes et al. 2019
pOGG0253	Rlv3841 *nifH* promoter driving *gusA* in stable RK2 plasmid; Nm^R	Geddes et al. 2019
pOGG0254	Rlv3841 *nifH* promoter driving *gusA* in stable RK2 plasmid; Nm^R	Geddes et al. 2019

pJG592	I-SceI meganuclease in pRK7813; Tc^R	Gift from Joel Griffiths
pAGE1.0	BAC/YAC multi-host shuttle vector with *oriT*, *S. meliloti* pSymA *repABC*; HIS3, Sp^R	Brumwell et al. 2019
pAGE2.0	BAC/YAC multi-host shuttle vector with *oriT*, *S. meliloti* pSymA *repABC*; HIS3, Tc^R	Brumwell et al. 2019
pAGE3.0	BAC/YAC multi-host shuttle vector with *oriT*, *S. meliloti* pSymA *repABC*; HIS3, Nm^R	Brumwell et al. 2019
pTH1522	Reporter vector containing a FRT site, ColE1 *oriV*; Gm^R	Cowie et al. 2006
pTH1496	pSymA incα in pOT1; Gm^R	MacLellan et al. 2005
pTH1937	ΔTn903 inverted repeats, pRK2 oriT, *nptII* from Tn5, p15A *oriV*; Nm^R	Milunovic et al. 2014
pTH1944	*flp* gene in a pBBR-MCS3 derivative with RK2-tetR-tetA; Tc^R	Milunovic et al. 2014
pTH2505	*flp* gene controlled by protocatechuate inducible promoter in pRK7813; Tc^R	Zhang et al. 2012
pTH2919	Tc^R *sacB* suicide vector, derived from pJQ200mp18; Tc^R	diCenzo and Finan 2015
pTH2992	pTH1496 (pOT1 with pSymA incα) with I-SceI cut site; Gm^R	Lab collection
pTH2993	pTrcSC expression vector with 3 pSymA antitoxins and I-SceI cut site; Gm^R	Lab collection
pTH3237	pTH2919 (pSymA nt 506,533-507,338 + 623,673-624,173 *via* XmaI/PstI); Tc^R	This work
pTH3255	A117-A118-A121 excised from pSymA of RmP4310 by Flp/FRT recombination, used to create minSymA1.0; Gm^R Nm^R	This work
pTH3278	fix-1 locus (pSymA nt 662,568-675,117) assembled by yeast recombineering in pAGE3.0 via ClaI/I-SceI; Nm^R	This work
pTH3291	pTH1522 3447 bp amplicon including oriV/oriT, FRT site and Gm^R, circularized via BglII; Gm^R	This work
pTH3294	nif-1/fix-3/syr/nif-2/nod-2/nol loci (pSymA nt 441,274-464,352, 465,636-474,959, 476,839-492,522) assembled into pTH3278 via I-SceI; Nm^R	This work
pTH3311	pTH1937 with pSymA nt 399,264-400,266 via KpnI/HindIII; Nm^R	This work
pTH3312	pTH1937 with pSymA nt 422,708-423,453 via KpnI/HindIII; Nm^R	This work
pTH3313	pTH1937 with pSymA nt 464,353-465,115 via KpnI/HindIII; Nm^R	This work
pTH3314	pTH1937 with pSymA nt 475,233-476,084 via KpnI/HindIII; Nm^R	This work
pTH3315	pTH3291 with pSymA nt 423,454-424,384 via BglII/PstI; Gm^R	This work
pTH3316	pTH3291 with pSymA nt 465,116-465,812 via BglII/PstI; Gm^R	This work
pTH3317	pTH3291 with pSymA nt 476,085-476,839 via BglII/PstI; Gm^R	This work
pTH3318	pTH3291 with pSymA nt 507,339-508,595 via BglII/PstI; Gm^R	This work
pTH3362	pOGG024 with chrom. nt 256,639-257,195, PnifH:: *gusA*, and chrom. nt 257,274-257,640 assembled by Golden Gate cloning via BsaI; Gm^R	This work
pTH3363	pOGG024 with chrom. nt 256,639-257,195, PnifH:: *celB*, and chrom. nt 257,274-257,640 assembled by Golden Gate cloning via BsaI; Gm^R	This work
pTH3364	Three fragment insert from pTH3362 cloned into pJQ200SK via XbaI/PstI; Gm^R	This work
pTH3365	Three fragment insert from pTH3362 cloned into pJQ200SK via XbaI/PstI; Gm^R	This work
pTH3369	pAGE1.0 with FRT and attP replacing *repABC* via ClaI/I-SceI; Sp^R	This work
pTH3370	pAGE2.0 with FRT and attP replacing *repABC* via ClaI/I-SceI; Tc^R	This work
pTH3371	synth-nod cluster (pSymA nt 418,096-422,417, 468,075-475,645, 477,027-	This work

	482,783, 485,141-492,308) assembled by yeast recombineering into pTH3369 via PacI; Sp^R	
pTH3372	fix-2 locus (pSymA nt 408,765-422,417) assembled by yeast recombineering into pTH3369 via PacI; Sp^R	This work
pTH3373	synth-nif cluster (pSymA nt 445,513-461,184, 482,759-485,097) assembled by yeast recombineering into pTH3370 via PacI; Tc^R	This work
pTH3375	synth-nod (pSymA nt 418,096-422,417, 468,075-475,645, 477,027-482,783, 485,141-492,308) and synth-nif (pSymA nt 445,513-461,184, 482,759-485,097) clusters assembled into pTH3278 via I-SceI; Nm^R	This work
pTH3376	synth-fix cluster created by assembling fix-2 locus (pSymA nt 412,309-417,593) with fix-1 locus in pTH3278 by yeast recombineering via I-SceI; Nm^R	This work
pTH3396	fix-2 locus *fix* genes (pSymA nt 412,309-417,593) assembled into pTH3369 via Pac-I; Sp^R	This work
pTH3434	NGR234 *nod* loci (pNGR234a nt 43,561-51,762; 312,667-316,686; 434,093-444,379; 495,184-497,027; 99,596-101,584) assembled into pTH3369 via Pac1; Sp^R	This work

*In all cases Nm^R refers to Nm^R (used for selection in *S. meliloti*) and Km^R (used for selection in *E. coli*)

Table S3. Primer sets used for amplification of symbiotic clusters

Plasmid	Vector		Forward Primer	Reverse Primer	pSymA location
pTH3278 (fix-1)	pAGE3.0 (Cla-I/ I-SceI)	1	GCTGTAAGTACATCACC GACGAGCAAGGCAAGA CGATCATATAACTTCGT ATAAAGTATCCTATACG AAGTTATCATGCCACCA GTCTAGCG	CGCAGACTTGACGCAG ATC	662,568-667,217
		2	CGATGTGCACGCTGTTC A	TGACCAACCTGCTAGC GTG	667,177-670,907
		3	GTGCTTTGGAACTCGCG A	GCCCAGCGGCGAGGGC AACCAGCTCGACTATA TTACCCTGTTATCCCTA GCGTAACTGAAGTTCCT ATACTTTCTAGAGAATA GGAACTTCGAACGCGA TTTGAATGCAGAA	670,869-675,117
pTH3294 (minSym2)	pTH3278 (I-SceI)	1	TCTCTAGAAAGTATAGG AACTTCAGTTACGCTAG GGATAAGCGCGACGAGC GAATTGC	TGGTCGATCCGCGTGTC G	441,274-445,137
		2	ATCCAGGGGTAGATCTT TACGC	CACCGGGATGCACTAC CG	445,098-449,102
		3	CACCTCATTGAAATCGT CTGACC	TTTGCGACCGTGCGCCT G	449,063-452,931
		4	AGAAGACAGGTGTCGAT ATCGC	ACTCCCATCAAATTGA GCAGGC	452,892-456,881
		5	GAACAATCGCGAGTTGA AGCG	CAAATATGGATGAGTT CGCGC	456,840-460,623
		6	CAACGATGCGGTCGCAG TG	ATGCCTGAAGTCACTA GGGCCCTTTATCTGACT ATCGGAGCG	460,585-464,352
		7	CTCCGATAGTCAGATAA AGGCGCTGGATGAAAAG TTCAG	GATCATACCGGCCTTG GAGG	465,636-472,075
		8	AGGCCAGACCAATTACT GCG	ATGGCCGGTAGTGCGG TGATCGCAATGTCCCGC TCGGC	472,055-474,959
		9	TCGCCGAGCGGGACATT GCGATCACCGCACTACC GGCC	CGCCAGGTACATTGATT GAACG	476,839-480,973
		10	CATAGCTCCGATCCGTT CCG	ATGCACCCGCCATCGG AG	480,955-485,122
		11	CTGTTTCCTAGGAGTATT CGCG	GCGGAATGTTCACCAT CGGC	485,083-489,130
		12	TGGTCGTCTACTCTTAG ATCGC	AGCGGCGAGGGCAACC AGCTCGACTATATTACC CTGTTATCCCTAACCGG AAAGGCTCCGGAC	489,091-492,522
pTH3372 (fix-2)	pTH3369 (Pac-I)	1	GTTTACAAGCATAAAGC TTGCTCAATCAATCACC GGATCCTTAATTAAGCG GAATCTTCTTGCTGTCA	CGCTCCTTCAGTTTCGT C	408,765-413,349

		2	GGACTATCTTGGCCTGAC	TCAGCCCCATGATCTCGG	413,290-418,112
		3	CAAACGCGCGCAACTC	CTATAATGACCCCGAAGCAGGGTTATGCAGCGGAAGATTTAATTAAGCTGAAGCGATGAGTCC	418,071-422,417
pTH3375 (minSym3)	pTH3278 (I-SceI)	1	TCTCTAGAAAGTATAGGAACTTCAGTTACGCTAGGGATAACGAGATCATGGGGCTGA	CATGGACGGAAAGGGACCGATGCCTGAAGTGCTGAAGCGATGAGTCC	418,096-422,417
		2	CGCCTGCATCGGCGGACTCATCGCTTCAGCACTTCAGGCATCGGTCC	CCTCCTATGGCTCCTGATG	468,075-471,673
		3	ATGTTCGAATTGACCGGGC	CTCACGCTTGGAAACAGCGATGAGAAGGCCCTCACTTCTCAGCAAGGCG	471,615-475,635
		4	CCGAGGAGGGCCGCCTTGCTGAGAAGTGAGGGCCTTCTCATCGCTGT	GTCCATTGCAGACCAGGAT	477,027-480,080
		5	TTCCGAGAACCATCATCAACG	GAGTATCGCTGGCAGCTTGATGAAGGTGCAAGCGAGGAGTTCTTGATCAAC	480,015-482,783
		6	AACTTGCATGTTGATCAAGAACTCCTCGCTTGCACCTTCATCAAGCTG	TGTCGATCACTACCCCGA	485,141-488,760
		7	TCGCGACCACTACGACT	TTCCCATCATCGAGCGACCGTCGGACGTGTGCCAAAC	488,714-492,308
		8	GCGGTTTGGCACACGTCCGACGGTCGCTCGATGATG	CCGACTGTCAATACGCATACC	443,513-447,635
		9	ACAGACAGGGCACTAACTC	CCAGCGATAATGAGGAGCG	447,537-452,213
		10	TCCTCCCGATCCTCAACG	CCGTGCAAGTCGTCACC	452,156-456,632
		11	CTTATAAGCTCTACGATCCGAAG	AGAAAAGCGAGGAGTTCTTGATCAACATGCCGTTCTACCGGTTCTTCTG	456,554-461,184
		12	GCGTGATCGGACAGAAGAACCGGTAGAACGGCATGTTGATCAAGAACTCCT	CCCAGCGGCGAGGGCAACCAGCTCGACTATATTACCCTGACTCCTAGGAAACAGATCACG	482,759-485,097
pTH3371 (synth-nod)	pTH3369 (Pac-I)	1	CAAGCATAAAGCTTGCTCAATCAATCACCGGATCCTTAATTAACGAGATCATGGGGCTGA	CATGGACGGAAAGGGACCGATGCCTGAAGTGCTGAAGCGATGAGTCC	418,096-422,417
		2	CGCCTGCATCGGCGGACTCATCGCTTCAGCACTTCAGGCATCGGTCC	CCTCCTATGGCTCCTGATG	468,075-471,673
		3	ATGTTCGAATTGACCGGGC	CTCACGCTTGGAAACAGCGATGAGAAGGCCCTCACTTCTCAGCAAGGC	471,615-475,635

				G	
		4	CCGAGGAGGGCCGCCTTGCTGAGAAGTGAGGGCCTTCTCATCGCTGT	GTCCATTGCAGACCAGGAT	477,027-480,080
		5	TTCCGAGAACCATCATCAACG	GAGTATCGCTGGCAGCTTGATGAAGGTGCAAGCGAGGAGTTCTTGATCAAC	480,015-482,783
		6	AACTTGCATGTTGATCAAGAACTCCTCGCTTGCACCTTCATCAAGCTG	TGTCGATCACTACCCCGA	485,141-488,760
		7	TCGCGACCACTACGACT	TAATGACCCCGAAGCAGGGTTATGCAGCGGAAGATTTAATTAATCGGACGTGTGCCAAAC	488,714-492,308
pTH3373 (synth-nif)	pTH3370 (Pac-I)	1	GACGCCGATGATTTGAAGCGCACTCAGCGTCTGATCTTAATTAACGGTCGCTCGATGATG	CCGACTGTCAATACGCATACC	443,513-447,635
		2	ACAGACAGGGCACTAACTC	CCAGCGATAATGAGGAGCG	447,537-452,213
		3	TCCTCCCGATCCTCAACG	CCGTGCAAGTCGTCACC	452,156-456,632
		4	CTTATAAGCTCTACGATCCGAAG	AGAAAAGCGAGGAGTTCTTGATCAACATGCCGTTCTACCGGTTCTTCTG	456,554-461,184
		5	GCGTGATCGGACAGAAGAACCGGTAGAACGGCATGTTGATCAAGAACTCCT	TCGCTATAATGACCCCGAAGCAGGGTTATGCAGCGGAAGATTTAATTAAACTCCTAGGAAACAGATCACG	482,759-485,097
pTH3396 (fix-2 reduced)	pTH3369 (Pac-I)	1	CTATTCTCTAGAAAGTATAGGAACTTCAGTTACGCTAGGGGCTTAATGGCGGCTCGTTG	AGCGGCGAGGGCAACCAGCTCGACTATATTACCCTGTTATCCCTAGATCTCGTATCCGCTACTC	412,309-417,593
pTH3376 (synth-fix)	pAGE3.0 (Cla-I/ I-SceI)	1	AGCATAAAGCTTGCTCAATCAATCACCGGATCCTTAATTAAGCTTAATGGCGGCTCGTTG	CTATAATGACCCCGAAGCAGGGTTATGCAGCGGAAGATGATCTCGTATCCGCTACTC	412,309-417,593
pTH3398 (stachy)	pTH3370 (Pac-I)	1	AGCAGGACCCGATGATTTGAAGCGCACTCAGCGTCTGATCCTCAGTTGATCACCAGCGG	AATGACCCCGAAGCAGGGTTATGCAGCGGAAGATTTAATTAACGCCTCGATTATGCTGCC	402,812-408,115
pTH3434 (NGR234 *nod*)	pTH3369 (Pac-I)	1	CAAGCATAAAGCTTGCTCAATCAATCACCGGATCCTTAATTAAGAGCCGACCGTGCAGTT	AAGACCTCAGATCGGCCTAC	43,561-47,513 (pNGR234a)
		2	GGAAGGTCATGGCGCAAA	GGCGATCAGGATGAGACGGCGCCTTAATTATCAGCCACATTGC	47,466-51,762 (pNGR234a)
		3	ATGTGGCTGATAATTAA	AAGTTGGATCAAAGAA	312,667-316,686

			GGCGCCGTCTCATCCTG ATCG	CAGGGACATACACGTA TCTTGCGCG	(pNGR234a)
		4	GCGCAAGATACGTGTAT GTCCCTGTTCTTTGATCC AACTTCC	TGTGCTCCGACTGAATT TAGT	434,093-439,036 (pNGR234a)
		5	GCTGTCCTGACCTACGG	ACCAGGGGCACGGATC AACACCTATTTTGTGAG GCTCTGCT	438,968-444,279 (pNGR234a)
		6	GCAGAGCCTCACAAAAT AGGTGTTGATCCGTGCC CCTG	GACGATTAGTGCATGT ATCCCGGCGCGTCAAA GATCG	495,184-497,027 (pNGR234a)
		7	AGGCGATCTTTGACGCG CCGGGATACATGCACTA ATCGTCAC	TAATGACCCCGAAGCA GGGTTATGCAGCGGAA GATTTAATTAACGCGAT GTCAAGCTCCT	99,596-101,584 (pNGR234a)

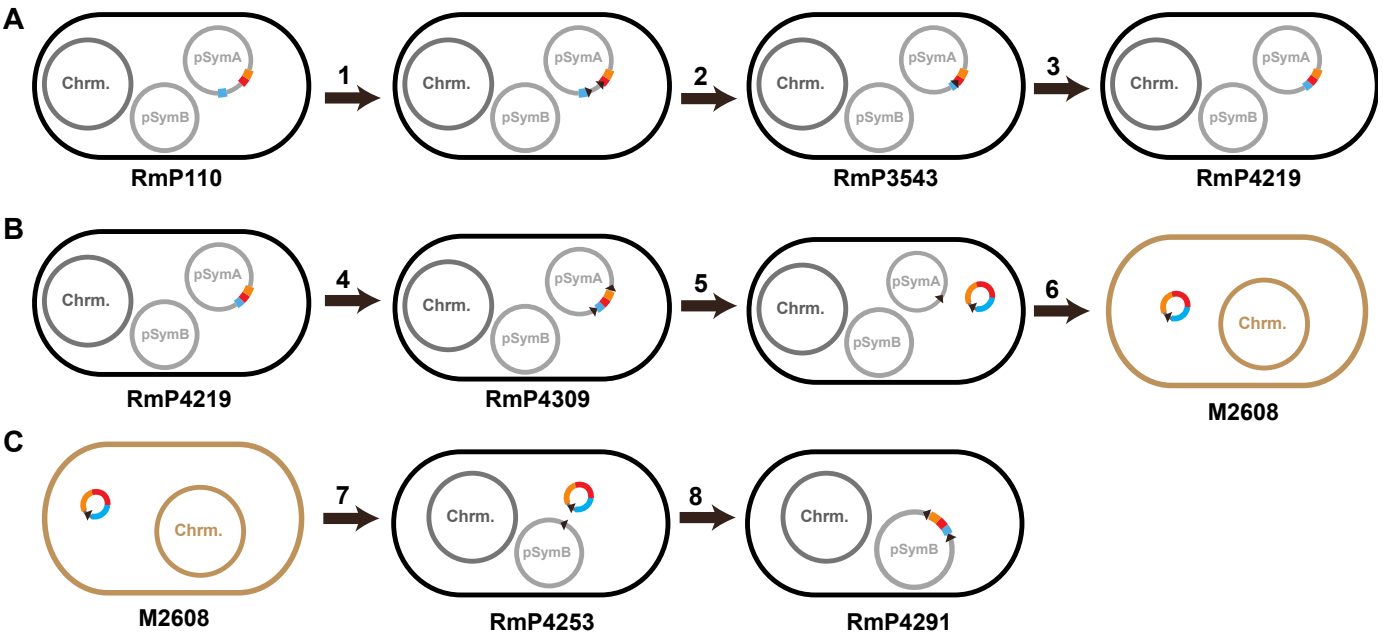

Figure S1. Schematic of symbiotic region capture and integration into a ΔpSymA background. A. Combination of essential regions into a single locus. Three separate regions were brought adjacent to one another by introducing *FRT* sites (black arrowheads) upstream of A121 (blue) and downstream of A118 (red)/A117 (orange) (1), deleting the intervening region by Flp-*FRT* recombination (2), and removing the *FRT* scar between the loci by double homologous recombination (3) to produce RmP4219. **B.** Isolation of A117-A118-A121 by *in vivo* region capture. *FRT* sites inside suicide plasmid backbones were introduced that flanked A117-A118-A121 (4), Flp-*FRT* recombination between *FRT*s excised the region as a plasmid capable of replicating in *E. coli* (5), and this plasmid was captured in *E. coli* by conjugation (6). **C.** Integration of A117-A118-A121 into pSymB to produce minSymA1.0. A117-A118-A121 were introduced to *S. meliloti* ΔpSymA as a suicide plasmid by conjugation (7), and integrated into an *FRT* site landing pad (*hypRE*::*FRT*) in pSymB by Flp-*FRT* recombination (8).

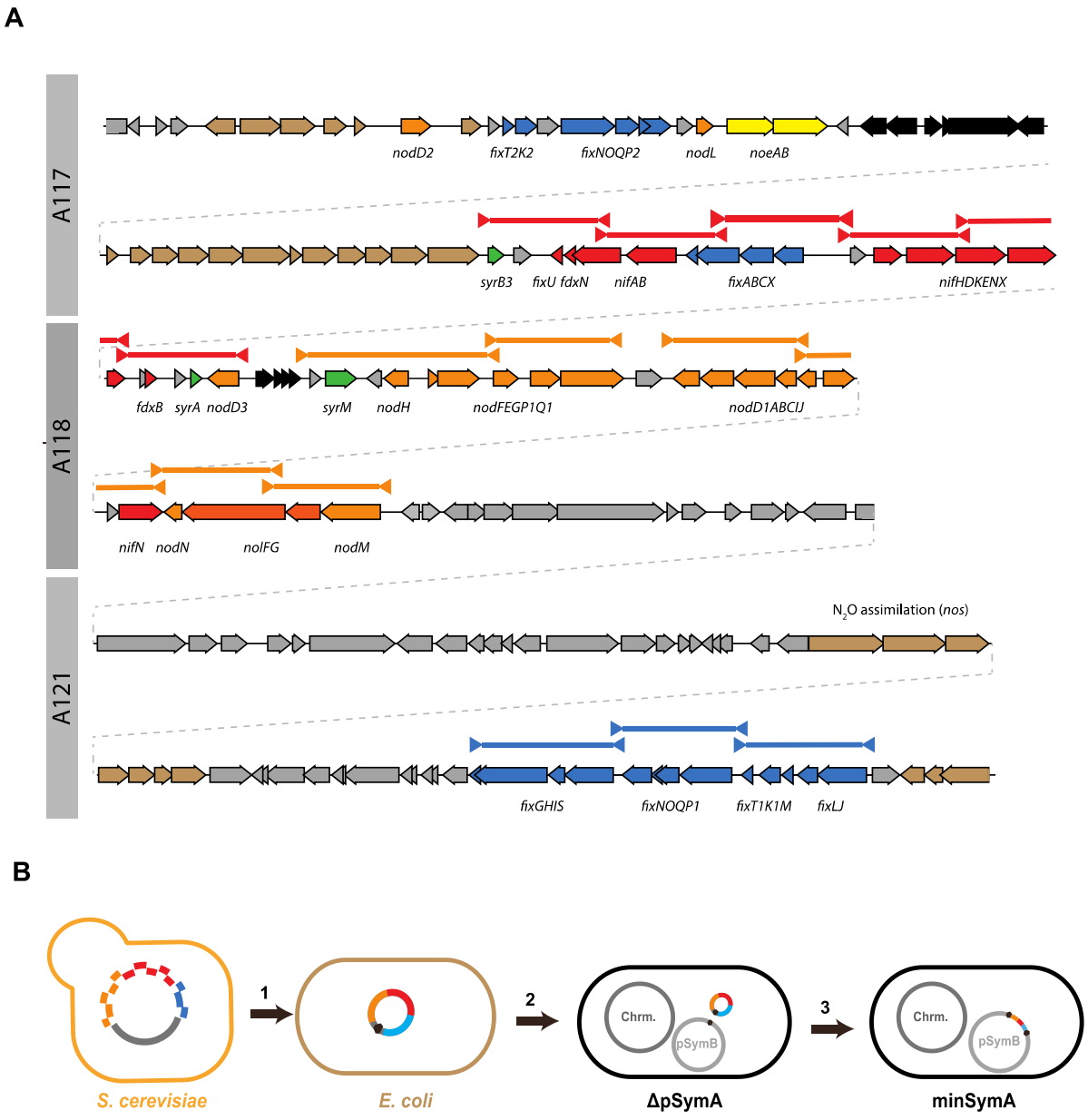

Figure S2. Schematic for assembly of symbiotic loci by yeast recombineering and integration into ΔpSymA. A. Loci of interest were amplified from a plasmid stock of pTH3255 (used to create minSymA1.0) by PCR. Shown are the amplicons used to assemble the symbiotic loci for construction of minSymA2.0. Amplified fragments were transformed with a compatible, linearized vector into *S. cerevisiae*. **B.** A circular plasmid is assembled from PCR amplicons and linearized vector backbone in *S. cerevisiae* by homologous recombination. The plasmid is isolated and introduced to *E. coli* by transformation (1). The suicide plasmid is introduced to *S. meliloti* ΔpSymA as a suicide plasmid by conjugation (2) and integrated into an *FRT* site landing pad in pSymB by Flp-*FRT* recombination (3).

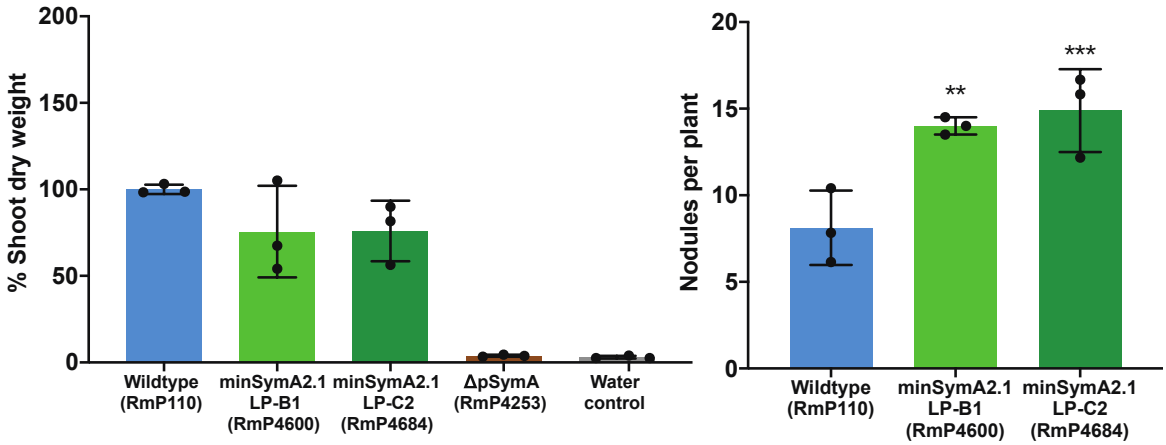

Figure S3. Genomic location does not influence symbiotic phenotypes. Shoot dry weight and nodules per plant are indicated for alfalfa inoculated with minSymA2.1 strains, with the minSymA2.0 complement of symbiotic genes integrated into either the LP-B1 (in pSymB) or LP-C2 (in the chromosome) landing pad (measurements from plants 38 days post inoculation). Statistical significance was assessed with one-way ANOVA and Dunnett's multiple comparisons test and is presented compared to wildtype. ** = P<0.01, ***= P<0.001.

Figure S4. *Medicago sativa* inoculated with minSymA1.0, minSymA2.1, and minSymA3.2. Images for representative plants from the three minimal genomes inoculated onto alfalfa with a ΔpSymA negative control are presented (31 days post inoculation). Scale bar represents 2 cm.

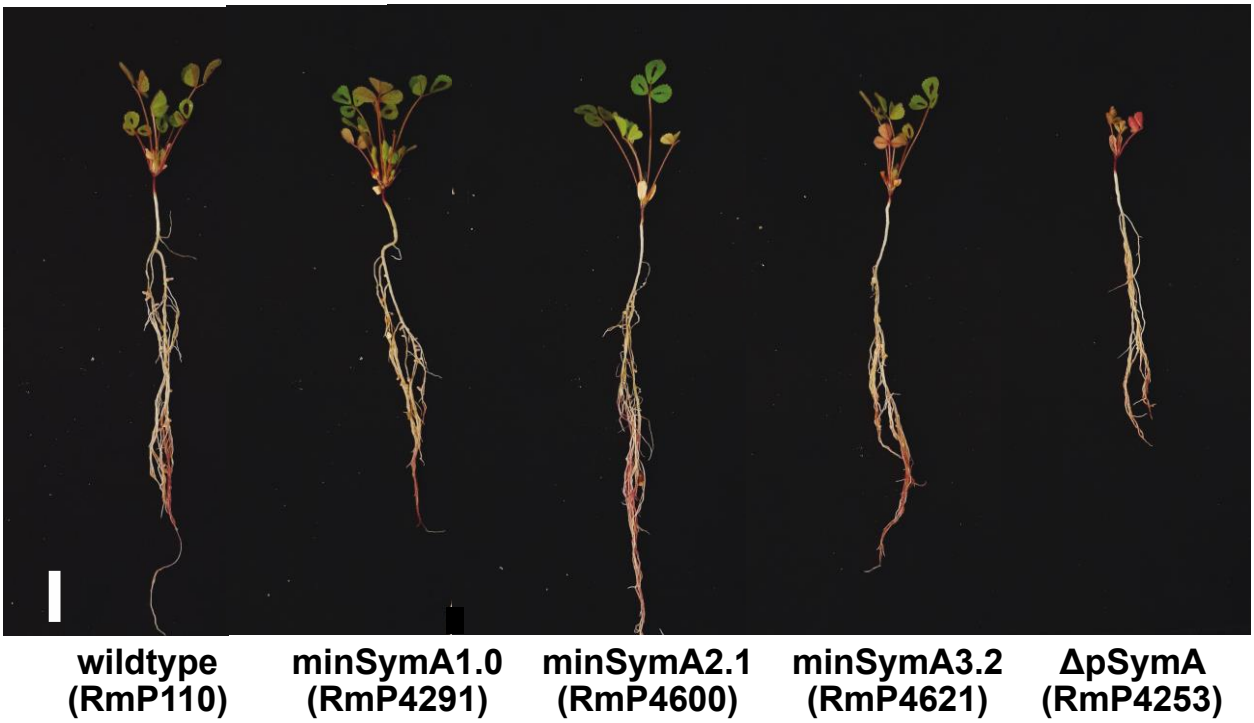

Figure S5. *Medicago truncatula* inoculated with minSymA1.0, minSymA2.1, and minSymA3.2. Images for representative plants from the three minimal genomes inoculated onto *M. truncatula* with a ΔpSymA negative control are presented (31 days post inoculation). Scale bar represents 2 cm.

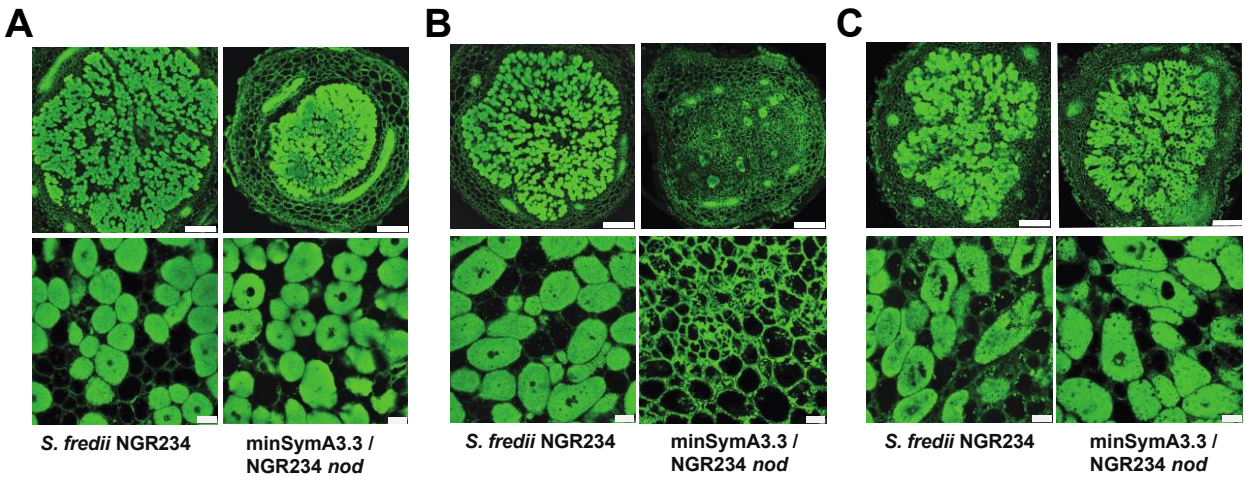

Figure S6. Confocal microscopy of nodules from *S. frediii* NGR234 hosts plants. Representative nodules from *Vigna unguiculata* (**A**), *Macroptilium aptropurpureum* (**B**) and *Leucaena leucocephala* (**C**) inoculated with wildtype *Sinorhizobium fredii* NGR234 or *Sinorhizobium meliloti* minSymA3.3 with the NGR234 *nod* cluster. Top panels show the whole nodule view with scale bar (white) representing 250 μm. The bottom panels provide a higher magnification view of the central portion of the nodules, with the scale bar (white) representing 25 μm.

SI References

1. H. M. Meade, S. R. Long, G. B. Ruvkun, S. E. Brown, F. M. Ausubel, Physical and genetic characterization of symbiotic and auxotrophic mutants of *Rhizobium meliloti* induced by transposon Tn*5* mutagenesis. *J. Bacteriol*. 149, 114–122 (1982).

2. I. J. Oresnik, T. C. Charles, T. M. Finan, Second site mutations specifically suppress the Fix- phenotype of *Rhizobium meliloti ndvF* mutations on alfalfa: identification of a conditional *ndvF*-dependent mucoid colony phenotype. *Genetics* 136, 1233–1243 (1994).

3. Z.-C. Yuan, R. Zaheer, T. M. Finan, Regulation and properties of PstSCAB, a high-affinity, high-velocity phosphate transport system of *Sinorhizobium meliloti*. *J. Bacteriol*. 188, 1089–1102 (2006).

4. B. Milunovic, R. A. Morton, T. M. Finan, Cell growth inhibition upon deletion of four toxin-antitoxin loci from the megaplasmids of *Sinorhizobium meliloti*. *J. Bacteriol*. 196, 811–824 (2014).

5. K. Kibitkin, "Transport and metabolism of β-glycosidic sugars in *Sinorhizobium meliloti*," McMaster University. (2011).

6. C. White, J. M. Gavina, R. Morton, P. Britz-McKibbin, T. M. Finan, Control of hydroxyproline catabolism in *Sinorhizobium meliloti*. *Mol. Microbiol*. 85, 1133–1147 (2012).

7. G. C. diCenzo, M. Zamani, B. Milunovic, T. M. Finan, Genomic resources for identification of the minimal N_2-fixing symbiotic genome. *Environ. Microbiol.* 18, 2534–2547 (2016).

8. T. M. Finan, B. Kunkel, G. F. de Vos, E. R. Signer, Second symbiotic megaplasmid in Rhizobium meliloti carrying exopolysaccharide and thiamine synthesis genes. *J. Bacteriol.* 167, 66–72 (1986).

9. J. Quandt, M. F. Hynes, Versatile suicide vectors which allow direct selection for gene replacement in Gram negative bacteria. *Gene* 127, 15–21 (1993).

10. B. A. Geddes, M. A. Mendoza-Suárez, P. S. Poole, A bacterial expression vector archive (BEVA) for flexible modular assembly of Golden Gate-compatible vectors. *Front. Microbiol.* 9, 3345 (2019).

11. S. L. Brumwell, *et al.*, Designer *Sinorhizobium meliloti* strains and multi-functional vectors enable direct inter-kingdom DNA transfer. *PLoS One* **14**, e0206781 (2019).

12. A. Cowie, *et al.*, An integrated approach to functional genomics: construction of a

novel reporter gene fusion library for *Sinorhizobium meliloti*. *Appl. Environ. Microbiol.* 72, 7156–7167 (2006).

13. Y. Zhang, T. Aono, P. Poole, T. M. Finan, NAD(P)+-malic enzyme mutants of *Sinorhizobium* sp. strain NGR234, but not *Azorhizobium caulinodans* ORS571, maintain symbiotic N2 fixation capabilities. *Appl Environ Microbiol* 78, 2803–2812 (2012).